Neural Computation with Spiking Neural Networks Composed of Synfire Rings

Jérémie Cabessa[1(✉)], Ginette Horcholle-Bossavit[2,3], and Brigitte Quenet[2,3]

[1] Laboratoire d'économie mathématique (LEMMA), Université Paris 2, Panthéon-Assas, Paris, France
jeremie.cabessa@u-paris2.fr

[2] Équipe de Statistique Appliquée, PSL Research University, ESPCI-ParisTech, Paris, France

[3] Neurophysiologie respiratoire expérimentale et clinique, Sorbonne Universités, UPMC Université Paris 6, INSERM, UMRS1158, Paris, France

Abstract. We show that any finite state automaton can be simulated by some neural network of Izhikevich spiking neurons composed of interconnected synfire rings. The construction turns out to be robust to the introduction of two kinds of synaptic noises. These considerations show that a biological paradigm of neural computation based on sustained activities of cell assemblies is indeed possible.

Keywords: Neural computation · Izhikevich spiking neurons · Synfire rings · Finite state automata

1 Introduction

In neural computation, the issue of the computational capabilities of neural networks is of central importance.

In this context, it has early been observed that Boolean recurrent neural networks are computationally equivalent to finite state automata [1–3]. These results opened the way to studies about simulations of finite automata by neural network models, with the aim of improving the implementation of finite state machines on parallel hardwares [4]. Nowadays, the computational power of diverse neural models have been shown to range from the finite automaton degree [1–4], up to the Turing [5,6] or even to the super-Turing level [7,8].

But from a biological perspective, the following question naturally arises: can the implementation of abstract machines be extended to the context of (more) biological neural networks? In fact, in biological nets, information is more likely processed by cell assemblies rather than by isolated entities [9,10], "mental states" are most probably represented by sustained activities of such assemblies rather than by specific spiking configurations, single neural connections are unreliable, and neural nets are subjected to various mechanisms of plasticity [11].

Along these lines, a novel paradigm of neural computation based on Boolean networks composed of synfire rings [9,10,12] has recently been proposed [13]. In

© Springer International Publishing AG 2017
A. Lintas et al. (Eds.): ICANN 2017, Part I, LNCS 10613, pp. 245–253, 2017.
https://doi.org/10.1007/978-3-319-68600-4_29

this paper, we show that this paradigm can be extended to the context of more biological neural networks, in accordance with the approach pursued in [14]. More precisely, we prove that any finite state automaton can be simulated by some neural network of Izhikevich spiking neurons [15] composed of interconnected synfire rings [12]. Furthermore, the obtained network is robust to the introduction of two kinds of synaptic noises. Our construction is general and can be realized for any finite state automaton. These considerations intend to show that a biological paradigm of neural computation based on sustained activities of cell assemblies is indeed possible.

2 Finite State Automata and Boolean Recurrent Neural Networks

Boolean recurrent neural networks are computationally equivalent to finite state automata [1–3]. On the one hand, any Boolean neural network can be simulated by some finite state automaton, and on the other hand, any finite automaton can be simulated by some Boolean network.

In Minsky's original construction [3] (known to be not optimal), a finite automaton with n states and k input symbols is simulated by a Boolean network whose cells are organized in a $k \times n$ grid. The grid structure displays one row and one column of cells per input symbol and computational state of the automaton, respectively. The weighted synaptic connections are suitably chosen in such a way that, if the automaton and its corresponding network are working in parallel on a same input stream, then the cell of location (i, j) in the network's grid will produce a spike if and only if the automaton is currently receiving the i-th input symbol and visiting the j-th computational state. In this precise sense, the computation of the original automaton is simulated by the spiking pattern

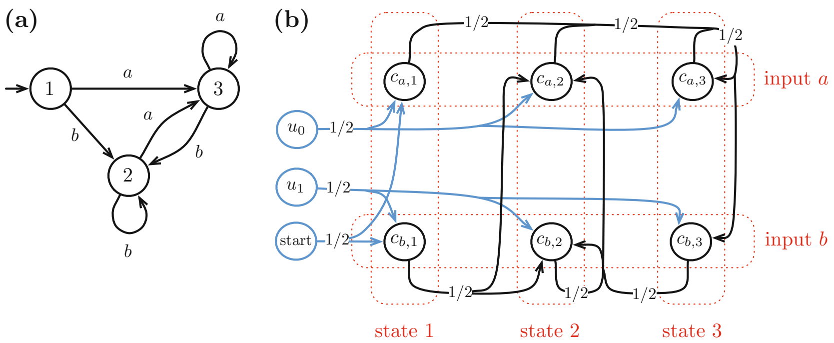

Fig. 1. Translation from a finite state automaton $\mathcal{A}$ (panel (a)) to an equivalent Boolean recurrent neural network $\mathcal{N}$ (panel (b)). The fact that $\mathcal{A}$ receives input a or b at time t is reflected by the input cells (u_0, u_1) of $\mathcal{N}$ taking values $(1, 0)$ or $(0, 1)$, respectively. The "start" cell spikes only at time $t = 0$ in order to initiate the dynamics.

Table 1. Simulation of automaton $\mathcal{A}$ of Fig. 1(a) by its corresponding network $\mathcal{N}$ of Fig. 1(b) and by its corresponding network of synfire rings $\mathcal{N}'$ of Fig. 3.

Inputs of $\mathcal{A}$	**a**	**b**	**a**	**a**	**a**	...
States of $\mathcal{A}$	**1**	**3**	**2**	**3**	**3**	...
Cell u_0 of $\mathcal{N}$	1	0	1	1	1	...
Cell u_1 of $\mathcal{N}$	0	1	0	0	0	...
Cell *start* of $\mathcal{N}$	1	0	0	0	0	...
Spiking cell of $\mathcal{N}$	–	$\mathbf{c_{a,1}}$	$\mathbf{c_{b,3}}$	$\mathbf{c_{a,2}}$	$\mathbf{c_{a,3}}$	$\mathbf{c_{a,3}}$
Active synfire ring of $\mathcal{N}'$	–	$\mathbf{R_{a,1}}$	$\mathbf{R_{b,3}}$	$\mathbf{R_{a,2}}$	$\mathbf{R_{a,3}}$	$\mathbf{R_{a,3}}$

of the corresponding network. This translation from a given finite automaton to its corresponding Boolean network is illustrated in Fig. 1.

A parallel simulation of the automaton and corresponding Boolean network of Fig. 1 is illustrated in Table 1. We see that the consecutive input symbols i and computational states j of $\mathcal{A}$ are correctly reflected by the sequence of spiking cells $c_{i,j}$ of $\mathcal{N}$, with a time delay of 1.

3 Finite State Automata and Boolean Networks of Synfire Rings

An alternative way of simulating finite state automata by means of Boolean recurrent neural networks made up of interconnected synfire rings has rencently been proposed [13]. The general idea consists in replacing each cell $c_{i,j}$ of the Boolean network of Fig. 1(b) by a synfire chain that loops back in on itself – referred to as a *synfire ring* $R_{i,j}$ [12] – illustrated in Fig. 2(a). In this way, each computational state of the original automaton will no more correspond to the punctual activity of a specific cell, but rather to the sustained activity of a specific synfire ring, that will persist until the appearance of the next input.

In order to complete the construction, the transitions between the various synfire rings shall correspond precisely to those between the cells of the network of Fig. 1(b). For this purpose, each excitatory connection between cells $c_{i,j}$ and $c_{i',j'}$ (black connections of Fig. 1(b)) is replaced by a fibre of excitatory connections between the corresponding synfire rings $R_{i,j}$ and $R_{i',j'}$ which connects every cells of $R_{i,j}$ to every cells of $R_{i',j'}$ (all-to-all connections). In addition, each synfire ring is associating with a so-called "triangular structure", illustrated in Fig. 2(b). This structure ensures that, every time a specific synfire ring is activated, it will inhibit all other rings, in order to remain the only one active, as explained in Fig. 2(b). Finally, weights of the input, intra-ring and inter-ring connections need to satisfy the following conditions:

(C1) The sole activity of the inter-ring connections does not suffice to activate any of the synfire ring.

(C2) The combined activity of the input cell and inter-ring connections is sufficiently large to activate the targeted synfire ring.

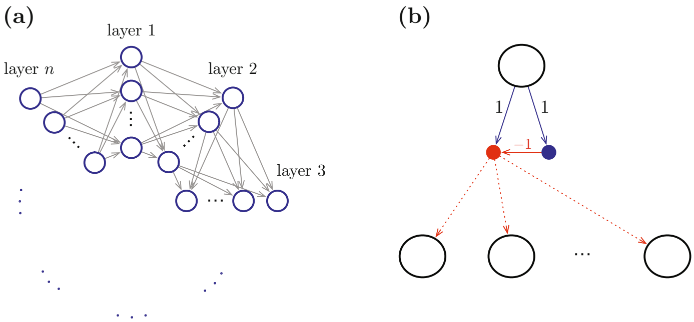

Fig. 2. (a) A synfire ring with n layers. Each cell of each layer is connected to all cells of the next layer. **(b)** The triangular structure associated to each synfire ring. Each large node represents a synfire ring and each little node represents a single cell. The two downward blue edges represent fibres of excitatory connections of weight 1 projecting from every cells of the upper ring to the blue and red units. The downward red edges represent fibres of sufficiently large inhibitory connections projecting from the red unit to every cells of the targeted synfire ring. If the upper ring fires at time t, it activates both red and blue cells at time $t+1$. Consequently, from time $t+2$ onwards, all other synfire rings, represented by the lower nodes, are inhibited via the red connections, and the red cell is also inhibited via the horizontal red connection. (Color figure online)

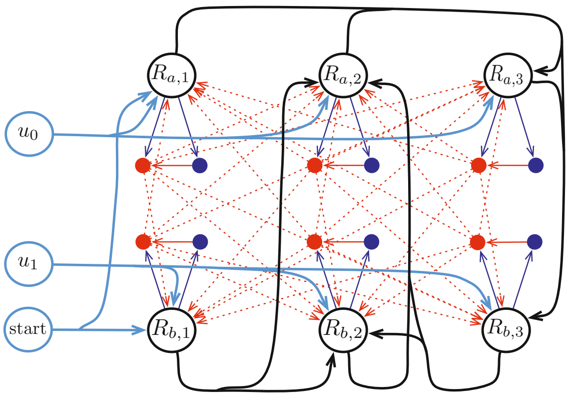

Fig. 3. Boolean recurrent neural network $\mathcal{N}'$ made up of interconnected synfire rings which simulates the automaton of Fig. 1(a). Each large node represents a synfire ring, as illustrated in Fig. 2(a). To each synfire ring is associated a triangular structure, as described in Fig. 2(b).

(C3) The inhibitory connections projecting from the triangular structures to the other synfire rings must be sufficiently negative to inhibit the total activity of the rings onto which they project.

The Boolean network of synfire rings associated to the automaton of Fig. 1 is illustrated in Fig. 3.

It was shown that every computation of the original automaton is correctly simulated by a corresponding sequence of sustained activities of synfire rings in the corresponding network [13]. More precisely, when the two systems are run in parallel on a same input stream, the synfire ring $R_{i,j}$ of the network – and only this one – will fire at a certain time step if and only if the automaton is currently receiving the i-th input symbol and visiting the j-th computational state. Moreover, the activity of that specific ring is self-sustained as long as no other input is received.

A parallel simulation of the automaton of Fig. 1(a) and its corresponding Boolean networks of synfire rings of Fig. 3 is illustrated in Table 1. We see that the consecutive input symbols i and computational states j of automaton $\mathcal{A}$ are correctly reflected by the sequence of active rings $R_{i,j}$ of network $\mathcal{N}'$.

The proposed construction can be applied to any finite state automaton. Consequently, the following result obtains [13]:

Theorem 1. *Any finite state automaton can be simulated by some Boolean neural network composed of interconnected synfire rings.*

4 Finite State Automata and Networks of Spiking Neurons

We show that the simulation of finite state automata by Boolean networks of synfire rings can be extended to the biological context of networks of spiking neurons.

More precisely, we consider a neural network made up of Izhikevich spiking neurons [15] with dimensionless parameters $a = 0.02, b = 0.2, c = -75, d = 0.4$ connected together by excitatory and inhibitory synapses with exponential decays of rates 0.3 and 0.2, respectively. The network contains the same architecture, i.e., the same input cells, synfire rings, and triangular structures as that of Fig. 3, but is subjected to a more complex dynamics defined by the differential equations of Izhikevich neurons [15]. Compared to the Boolean network of Sect. 3, the excitatory inter-rings connections needed to be considerably reduced (from 1.0 to 0.11), due to the combined activities of the neurons. The weight matrix of the network is given in Fig. 4 (left).

This network of spiking neurons was able to perfectly simulate the behavior of the automaton of Fig. 1(a), in the precise sense explained in Sect. 3. For instance, Fig. 5(a1) provides the raster plot of the network's activity where inputs a, b, a, a, a are provided at regular intervals of 625 ms. We see that, according to the sequence of inputs received, the network's activity successively switches from the groups of neurons $4-21$ to $104-121$ to $24-41$ to $44-61$ and to $44-61$ again, which corresponds precisely to the successive activations of the synfire rings $R_{a,1}, R_{b,3}, R_{a,2}, R_{a,3}, R_{a,3}$, as expected by the simulation process described in Table 1. We repeated the simulations with different input streams and during longer times, and the simulation process was always correct. It is worth noting that the network's dynamics shows the emergence of a regular temporal structure

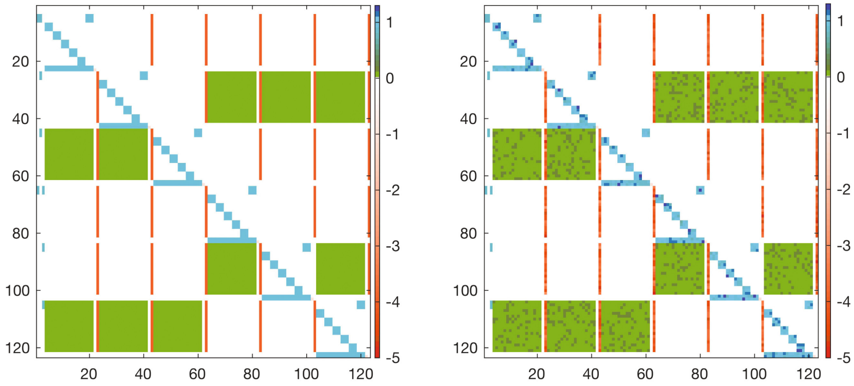

Fig. 4. Weight matrices of the network of Izhikevich neurons connected according to the architecture described in Fig. 3. The excitatory and inhibitory weights are expresses as percentages of the respective maximal synaptic strengths, set at 5.6 and 15.0. The left and right panel represent the matrix without and with the addition of synaptic noise, respectively. Neurons number 1, 2 and 3 are the *start*, u_0 and u_1 cells. Groups of neurons $4-21$, $24-41$, $44-61$, $64-81$, $84-101$ and $104-121$ represent the six synfire rings $R_{a,1}$, $R_{a,2}$, $R_{a,3}$, $R_{b,1}$, $R_{b,2}$ and $R_{b,3}$, respectively. Neurons $22-23$, $42-43$, $62-63$, $82-83$, $102-103$ and $122-123$ are the pairs of cells of the triangular structures associated to the six synfire rings. The blue regions represent the input and intra-ring connections; the green regions represent the inter-ring connections; the orange region are the inhibitory connections projecting from the triangular structures. (Color figure online)

induced by the synfire connectivity. Figure 5(a2) displays the synaptic current and membrane potential of neuron 10. We see that the neuron is spiking during the activation of the first synfire ring $R_{a,1}$. Afterwards, it remains quiet and endures the three successive massive inhibitions occurring at every switch of synfire ring activity.

Moreover, the simulation process turns out to be robust to the introduction of two kinds of synaptic noises. First, we perturbed the inter-ring, intra-ring and inhibitory connections with a centred Gaussian noise of about 10% of the original weights, as depicted in Fig. 4(left). The obtained noisy weight matrix is given in Fig. 4(right). Secondly, we introduced a dynamic synaptic noise (or membrane noise), by distorting the membrane current with a standard Gaussian noise at every updating step, as illustrated by the noisy black and magenta traces of Fig. 5(b2). Figure 5(b1) provides the raster plot of the network's activity subjected to these two kinds of synaptic noises, and shows that the simulation of the automaton is still correctly performed.

Besides, it is known that different kinds of neurons – e.g., Izhikevich thalamo-ortical (TC-IZH) [15], Izhikevich necortical regular-spiking (RS-IZH) [15], Izhikevich resonator (RZ-IZH) [15], exponential integrate-and-fire (RS-EIF) [16], multiple-timescale adaptive-threshold (RS-MAT) [17] – exhibit different properties in transmitting temporal information accurately and reliably when organized

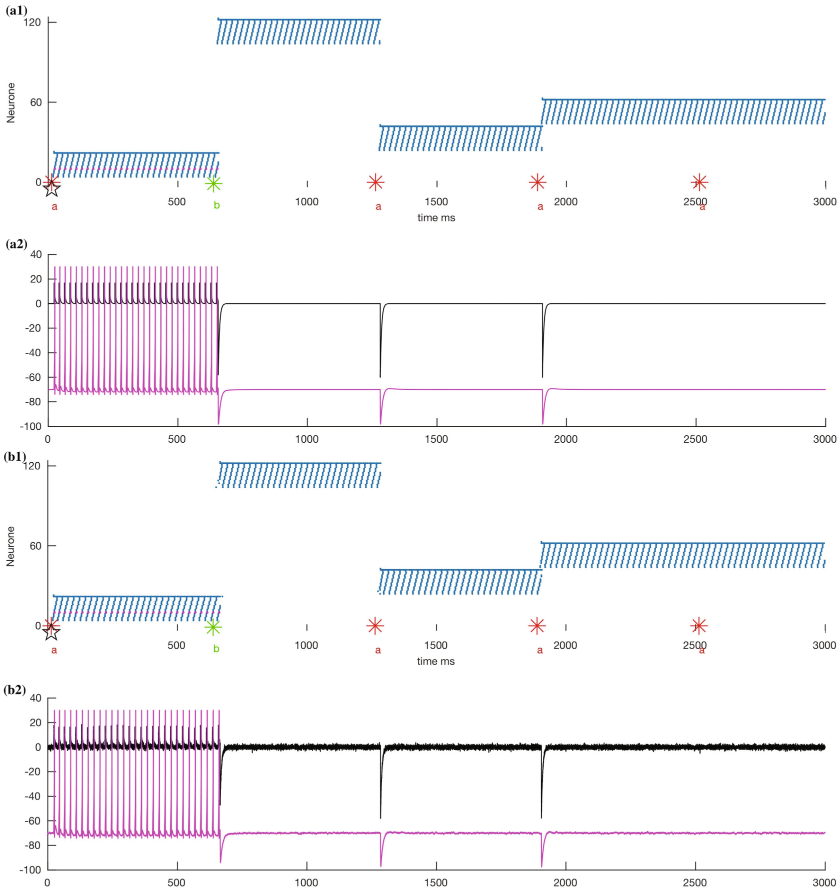

Fig. 5. (a1) Raster plot of the network's activity, when receiving the sequence of inputs a, b, a, a, a. **(b1)** Synaptic current (black) and membrane potential of neuron 10 (magenta) over time. **(a2)** Raster plot of the network's activity subjected to two kinds of synaptic noise, when receiving the sequence of inputs a, b, a, a, a. **(b2)** Synaptic current (black) and membrane potential of neuron 10 (magenta) over time, when the network is subjected to the two kinds of synaptic noises. (Color figure online)

either into simple chains [18] or into synfire chains [19]. Our network involves Izhikevich neurons whose dynamics resembles that of simple McCulloch and Pitts' cells. But by carefully tuning our synaptic connections, we were also able to correctly simulate the behavior of the finite automaton of Fig. 1(a) with networks of synfire rings composed of either TC-IZH or RS-IZH or RZ-IZH neurons (with dimensionless parameters $a = 0.02, b = 0.25, c = -65, d = 2$ or $a = 0.02, b = 0.2, c = -65, d = 8$ or $a = 0.1, b = 0.26, c = -65, d = 2$, respectively, cf. [18]), as well as with many other kinds of Izhikevich neurons. The synaptic weights of the networks composed of the three types of aforementioned neurons are given in Table 2.[1]

Table 2. Synaptic weights (s.w.) of three networks composed of three types of Izhikevich neurons, each of which correctly simulates the finite automaton of Fig. 1(a).

	TC-IZH	RS-IZH	RZ-IZH
Input s.w. (light blue Fig. 3)	0.45	1.11	0.1305
Intra-ring s.w. (grey Fig. 2(a))	0.8	1.83	0.8
Inter-ring s.w. (black Fig. 3)	0.049	0.09	0.02
Inhib. s.w. (dashed red Fig. 3)	−2.0	−6.0	−2.0
Triangle s.w. (dark blue & solid red Fig. 3)	1.0 & −1.1	1.0 & −2.0	1.0 & −1.1

Finally, note that the above construction is generic: it can be applied to any finite state automaton. Consequently, Theorem 1 can be extended to this more biological context.

Theorem 2. *Any finite state automaton can be simulated by some noisy neural network of Izhikevich spiking neurons composed of interconnected synfire rings.*

5 Conclusion

We showed that any finite state automaton can be simulated by some neural network of Izhikevich spiking neurons composed of interconnected synfire rings. Our construction turns out to be robust to two kinds of local synaptic noises as well as to the consideration of various types of Izhikevich neurons. This feature is based on the fact that the correctness of our simulation process does not rely on the processing of precise temporal information [18,19], but rather on simple activation and self-sustainability of specific synfire rings, which is a coarser feature. We however noticed that our construction turns out to be highly sensitive to global changes of the synaptic weights.

With these achievements, we do not intend to argue that brain computational processes really proceed via simulations of finite state automata in the very way that we described. Rather, our intention is to show that a bio-inspired paradigm of abstract neural computation based on sustained activities of neural assemblies is indeed possible, and potentially harnessable. As a consequence, biological neural networks should in principle be capable of simulating the abstract computational model represented by finite state automata, whether via the proposed paradigm, or via some other one.

For future work, we plan to extend these results to the Turing complete level of computation. Towards this purpose, the networks should be able to encode an

[1] For the case of RS-IZH neurons, the exponential decay's rate of the excitatory synapses has been changed from 0.3 to 0.4.

unbounded amount of information representing the possibly unbounded content of the Turing machine's infinite tape throughout the computational process. The biological plausibility of this feature is expected to be explored.

References

1. McCulloch, W.S., Pitts, W.: A logical calculus of the ideas immanent in nervous activity. Bull. Math. Biophys. **5**, 115–133 (1943)
2. Kleene, S.C.: Representation of events in nerve nets and finite automata. In: Shannon, C., McCarthy, J. (eds.) Automata Studies, pp. 3–41. Princeton University Press, Princeton (1956)
3. Minsky, M.L.: Computation: Finite and Infinite Machines. Prentice-Hall Inc., Englewood Cliffs (1967)
4. Siegelmann, H.T.: Recurrent neural networks and finite automata. Computat. Intell. **12**, 567–574 (1996)
5. Turing, A.M.: Intelligent machinery. Technical report, National Physical Laboratory, Teddington, UK (1948)
6. Siegelmann, H.T., Sontag, E.D.: On the computational power of neural nets. J. Comput. Syst. Sci. **50**(1), 132–150 (1995)
7. Siegelmann, H.T., Sontag, E.D.: Analog computation via neural networks. Theor. Comput. Sci. **131**(2), 331–360 (1994)
8. Cabessa, J., Siegelmann, H.T.: The super-Turing computational power of plastic recurrent neural networks. Int. J. Neural Syst. **24**(8), 1–22 (2014)
9. Abeles, M.: Local Cortical Circuits: An Electrophysiological Study. Studies of Brain Function, vol. 6. Springer, Heidelberg (1982)
10. Abeles, M.: Time is precious. Science **304**(5670), 523–524 (2004)
11. Abbott, L.F., Nelson, S.B.: Synaptic plasticity: taming the beast. Nat. Neurosci. **3**(Suppl), 1178–1183 (2000)
12. Zheng, P., Triesch, J.: Robust development of synfire chains from multiple plasticity mechanisms. Front. Comput. Neurosci. **8**, 66 (2014)
13. Cabessa, J., Masulli, P.: Emulation of finite state automata with networks of synfire rings. In: 2016 International Joint Conference on Neural Networks, IJCNN 2017, Anchorage, AK, USA, May 14–19, 2017 (2017, to appear)
14. Horcholle-Bossavit, G., Brigitte, Q.: Neural model of frog ventilatory rhythmogenesis. Biosystems **97**(1), 35–43 (2009)
15. Izhikevich, E.M.: Simple model of spiking neurons. IEEE Trans. Neur. Netw. **14**(6), 1569–1572 (2003)
16. Fourcaud-Trocmé, N., Hansel, D., van Vreeswijk, C., Brunel, N.: How spike generation mechanisms determine the neuronal response to fluctuating inputs. J. Neurosci. **23**(5), 11628–11640 (2003)
17. Kobayashi, R., Tsubo, Y., Shinomoto, S.: Made-to-order spiking neuron model equipped with a multi-timescale adaptive threshold. Front. Comput. Neurosci. **3**, 9 (2009)
18. Asai, Y., Guha, A., Villa, A.E.P.: Deterministic neural dynamics transmitted through neural networks. Neural Netw. **21**(6), 799–809 (2008)
19. Asai, Y., Villa, A.: Integration and transmission of distributed deterministic neural activity in feed-forward networks. Brain Res. **1434**, 17–33 (2012)